Experimental observation of Einstein-Podolsky-Rosen steering via entanglement detection

Huan Yang,[1,2,3] Zhi-Yong Ding,[1,4,5] Dong Wang,[1,6] Hao Yuan,[1,6,7] Xue-Ke Song,[1] Jie Yang,[1] Chang-Jin Zhang,[2] and Liu Ye[1,*]

[1]*School of Physics and Material Science, Anhui University, Hefei 230601, China*

[2]*Institutes of Physical Science and Information Technology, Anhui University, Hefei 230601, China*

[3]*Department of Experiment and Practical Training Management, West Anhui University, Luan 237012, China*

[4]*School of Physics and Electronic Engineering, Fuyang Normal University, Fuyang 236037, China*

[5]*Key Laboratory of Functional Materials and Devices for Informatics of Anhui Educational Institutions, Fuyang Normal University, Fuyang 236037, China*

[6]*CAS Key Laboratory of Quantum Information, University of Science and Technology of China, Hefei 230026, China*

[7]*Key Laboratory of Opto-Electronic Information Acquisition and Manipulation of Ministry of Education, Anhui University, Hefei 230601, China*

(Received 1 January 2020; revised manuscript received 20 March 2020; accepted 23 March 2020; published 16 April 2020)

The Einstein-Podolsky-Rosen (EPR) steering is an intermediate quantum nonlocality between entanglement and Bell nonlocality, which plays an important role in quantum information processing tasks. In the past few years, the investigations concerning the EPR steering have been demonstrated in a series of experiments. However, these studies rely on the relevant steering inequalities and the choices of measurement settings. Here, we experimentally verify the EPR steering via entanglement detection without using any steering inequality and measurement setting. By constructing two new states from a two-qubit state, we observe the EPR steering by detecting the entanglement of these new states. The results show that the entanglement of the newly constructed states can be regarded as an unusual kind of steering witness for these states. Compared to the results of Xiao *et al.* [Phys. Rev. Lett. **118**, 140404 (2017)], we find that the ability to detect the EPR steering in our scenario is stronger than that of two-setting projective measurements, which can observe more steerable states. Hence, our demonstrations can deepen the understanding of the connection between the EPR steering and entanglement.

DOI: 10.1103/PhysRevA.101.042115

I. INTRODUCTION

The investigations of the Einstein-Podolsky-Rosen (EPR) steering, which was considered as a "spooky" action permissible under the rules of quantum mechanics, can be traced back to 1935 [1,2]. Assuming two entangled parties shared by Alice and Bob in separated space, the EPR steering depicts a distinctive nonclassical trait that Alice can immediately steer the Bob's system by implementing a measurement on her system. Recently, Wiseman *et al.* rigorously and operationally defined the EPR steering as an information-theoretic task [3]. The EPR steering exists in the situation that the joint probabilities of measurement outcomes cannot be described by constructing a local-hidden-variable–local-hidden-state (LHV-LHS) model. The hierarchy of quantum nonlocalities, namely, steerable states are a strict subset of the entangled states [4] and a superset of Bell nonlocal states [5,6], was also provided [3]. The EPR steering can thus be regarded as an entanglement witness; i.e., there must be entanglement in a steerable state. In the past decade, the explorations concerning the EPR steering have attracted increasing attention since it has many potential applications in quantum information processing, for example, one-sided device-independent quantum key distribution [7–9], secure quantum teleportation [10,11], one-sided device-independent randomness generation [12], and so on.

The EPR steering can be detected by the violation of various steering inequalities, including linear steering inequalities [13,14], inequalities based on entropic uncertainty relations [15–18], the steering criterion from a geometric Bell-like inequality [19], and the steering inequality with tolerance for measurement-setting errors [20]. On the theory side, based on the choices of measurements, the EPR steering has been explored from projective measurements [21] to positive operator-valued measures (POVMs) [22–24], and also from continuous variable systems [25,26] to discrete systems [21,23,27].

Experimentally, the EPR steering was investigated by a few efforts in the past few years, and many significant results were demonstrated. Saunders *et al.* experimentally observed quantum steering for Bell local states via linear steering inequality [28] and demonstrated that the EPR steering occurs for mixed entangled states that are Bell local. Bennet *et al.* experimentally certified that the EPR steering can be rigorously implemented in the case of arbitrarily high losses [29]. The EPR steering of Gaussian states was verified by performing Gaussian measurements [30] and then was extended to a multipartite system [31]. By using the steering radius, Sun *et al.* [32] and Xiao *et al.* [33] explored the EPR steering in different directions through two-setting and multisetting projective measurements, respectively. The results show that

*yeliu@ahu.edu.cn

more states are shown to be steerable with the increase of measurement setting in experiments. Considering 16 measurements and a Werner state with a lossy channel at one side, Wollmann *et al.* observed the EPR steering in the general setting of POVMs [24]. Without assumption concerning the experimental state or measurement, Tischler *et al.* verified the asymmetry of the EPR steering in the situation of a two-qubit state with loss [34]. Also, Li *et al.* explored the EPR steering of a two-qubit Werner state via the geometric Bell-like steering inequality [35]. However, these experimental efforts rely on the relevant steering inequalities and the choices of measurement settings, which makes it difficult for them to avoid the locality loophole presented in the EPR steering tests. In general, an entangled state can be verified by detecting the EPR steering, and the converse is not always true [22]. The detection of the EPR steering is also strictly harder than the detection of entanglement [28]. Therefore, an open question is raised: can we realize the observation of the EPR steering by detecting the entanglement in experiments? That is still lacking, and the study may provide a way to test a difficultly detected quantum correlation by translating it into an easily detected problem.

In this paper, we demonstrate the EPR steering via detecting entanglement in experiments, without using any steering inequality and measurement setting. To be specific, we experimentally construct two new states from a two-qubit state on the basis of the recent theories of Das *et al.* [36] and Chen *et al.* [37], and we observe the EPR steering by detecting the entanglement of these states. The results verify that the entanglement of newly constructed states can be considered as an unusual kind of EPR steering witness for two-qubit states in experiments. These experimental results can deepen our understanding of the connection between steering and entanglement. We further compare our results with the ones of Xiao *et al.* [33], and it is shown that the ability to detect the EPR steering in our scenario is stronger than that of two-setting projective measurements.

II. OBSERVING THE EPR STEERING THROUGH ENTANGLEMENT DETECTION

Consider a bipartite quantum state ρ_{AB} shared by Alice and Bob, and the possible choices of measurements are A (measurement operators are denoted by M_a^A) and B (measurement operators are denoted by M_b^B) for Alice and Bob, respectively. Assuming that Alice obtains the measurement outcome a by carrying out the measurement of A on her subsystem, Bob obtains the corresponding outcome b by implementing the measurement B on his subsystem. If and only if the corresponding joint probability distribution of the outcomes cannot be expressed by $P(a,b|A,B,\rho_{AB}) = \sum_\lambda P(\lambda)P(a|A,\lambda)P_Q(b|B,\rho_\lambda)$, then ρ_{AB} is steerable from Alice to Bob [3]. Here, $P(\lambda)$ is the probability distribution over the LHVs λ satisfying $\sum_\lambda p(\lambda) = 1$. $P(a|A,\lambda)$ indicates a general probability distribution, and $P_Q(b|B,\rho_\lambda) = \mathrm{tr}[\rho_\lambda M_b^B]$ is the probability of outcome b performing measurement B on the LHS ρ_λ. In other words, ρ_{AB} can realize steering from Alice to Bob if and only if there is no LHV-LHS model described by the joint probability distribution for arbitrary measurements implemented by Alice and Bob.

Any bipartite separable state is defined as a convex mixture of product states, namely, $\rho_{AB} = \sum_\lambda p(\lambda)\rho_\lambda^A \otimes \rho_\lambda^B$. The state ρ_{AB} is entangled if and only if the joint probability distribution cannot be represented by $P(a,b|A,B,\rho_{AB}) = \sum_\lambda P(\lambda)P_Q(a|A,\rho_\lambda^A)P_Q(b|B,\rho_\lambda^B)$, where $P_Q(a|A,\rho_\lambda^A) = \mathrm{tr}[\rho_\lambda^A M_a^A]$ and $P_Q(b|B,\rho_\lambda^B) = \mathrm{tr}[\rho_\lambda^B M_b^B]$. That is, ρ_{AB} is an entangled state if and only if there is no LHS-LHS model described by this joint probability distribution for arbitrary measurements performed by Alice and Bob. Recently, Das *et al.* [36] and Chen *et al.* [37] proposed a criterion sufficient to detect the EPR steering for bipartite states through the entanglement detection of newly constructed states. In theory, for any two-qubit state ρ_{AB} shared by Alice and Bob, we can construct two new states as τ_{AB}^1 and τ_{AB}^2,

$$\tau_{AB}^1 = \mu_1\rho_{AB} + (1-\mu_1)\tilde{\rho}_{AB}^1 \tag{1}$$

and

$$\tau_{AB}^2 = \mu_2\rho_{AB} + (1-\mu_2)\tilde{\rho}_{AB}^2. \tag{2}$$

Here, $\tilde{\rho}_{AB}^1 = \rho_A \otimes \mathbb{I}/2$, $\rho_A = \mathrm{tr}_B[\rho_{AB}]$, $\tilde{\rho}_{AB}^2 = \mathbb{I}/2 \otimes \rho_B$, $\rho_B = \mathrm{tr}_A[\rho_{AB}]$, $\mu_1 \in [0, 1/\sqrt{3}]$, and $\mu_2 \in [0, 1/\sqrt{3}]$. If τ_{AB}^1 is an entangled state, then the state ρ_{AB} is steerable from Bob to Alice. In addition, if τ_{AB}^2 is entangled, then the steering task from Alice to Bob can be realized. It is important to mention here that whether the given state ρ_{AB} may be steerable from Bob to Alice (from Alice to Bob) is not certain when the newly constructed state τ_{AB}^1 (τ_{AB}^2) is separable. As a consequence, the unsteerability of ρ_{AB} cannot be demonstrated via detecting the entanglement of newly constructed states. In order to observe the EPR steering in experiment, the steerable states need to be prepared in our photon-polarization-qubit system. We focus our attention on a family of two-qubit states [38]:

$$\rho_{AB}(\alpha,\theta) = \alpha|\psi(\theta)\rangle\langle\psi(\theta)| + (1-\alpha)\mathbb{I}/2 \otimes \rho_B, \tag{3}$$

with $|\psi(\theta)\rangle = \cos(\theta)|HH\rangle + \sin(\theta)|VV\rangle$ and $\rho_B = \mathrm{tr}_A[|\psi(\theta)\rangle\langle\psi(\theta)|]$. Here, $0 \leqslant \alpha \leqslant 1$ and $0 \leqslant \theta \leqslant \pi/4$. The horizontally and vertically polarized components are represented by H and V, respectively. It is shown that the state is steerable from Alice to Bob if $\alpha > 1/2$. Moreover, it is demonstrated that Bob cannot steer Alice for $\cos^2(2\theta) \geqslant (2\alpha-1)/(2-\alpha)\alpha^3$ by employing the uniform distribution as an ansatz for the LHS ensemble [38]. According to Refs. [36,37], the newly constructed states $\tau_{AB}^1(\alpha,\theta)$ and $\tau_{AB}^2(\alpha,\theta)$ for $\rho_{AB}(\alpha,\theta)$ can be given by

$$\tau_{AB}^1(\alpha,\theta) = \mu_1\rho_{AB}(\alpha,\theta) + (1-\mu_1)\tilde{\rho}_{AB}^1(\alpha,\theta) \tag{4}$$

and

$$\tau_{AB}^2(\alpha,\theta) = \mu_2\rho_{AB}(\alpha,\theta) + (1-\mu_2)\tilde{\rho}_{AB}^2(\alpha,\theta), \tag{5}$$

where $\tilde{\rho}_{AB}^1(\alpha,\theta) = \rho_A(\alpha,\theta) \otimes \mathbb{I}/2$ with $\rho_A(\alpha,\theta) = \mathrm{tr}_B[\rho_{AB}(\alpha,\theta)]$, and $\tilde{\rho}_{AB}^2(\alpha,\theta) = \mathbb{I}/2 \otimes \rho_B(\alpha,\theta)$ with $\rho_B(\alpha,\theta) = \mathrm{tr}_A[\rho_{AB}(\alpha,\theta)]$. It is known that the entanglement of two-qubit states can be effectively identified by the concurrence [39]. The concurrence of ρ_{AB} is written as $C(\rho_{AB}) = \max\{0, \sqrt{\lambda_1} - \sqrt{\lambda_2} - \sqrt{\lambda_3} - \sqrt{\lambda_4}\}$, where λ_i $(i = 1,2,3,4)$ are the eigenvalues with decreasing order of the matrix $\rho_{AB}(\sigma_y \otimes \sigma_y)\rho_{AB}^*(\sigma_y \otimes \sigma_y)$. The variable ρ_{AB}^* represents the complex conjugate of ρ_{AB} in the fixed basis

$\{|00\rangle, |01\rangle, |10\rangle, |11\rangle\}$. By some calculations, the condition for the case that $\tau^1_{AB}(\alpha,\theta)$ is an entangled state (Bob can steer Alice) can be given by

$$\frac{\sqrt{3}-\sqrt{3}\cos(4\theta)-2\sqrt{7-4\cos(4\theta)+\cos^2(4\theta)}}{\cos(4\theta)-5} < \alpha \leqslant 1, \tag{6}$$

with $0 < \theta \leqslant \pi/4$. The condition of $\tau^2_{AB}(\alpha,\theta)$ being an entangled state (Alice can steer Bob) can be written as $1/\sqrt{3} < \alpha \leqslant 1$ and $0 < \theta \leqslant \pi/4$. Hence, to make sure that $\tau^2_{AB}(\alpha,\theta)$ is an entangled state and $\tau^1_{AB}(\alpha,\theta)$ is a separable state, it should satisfy the following condition:

$$\frac{1}{\sqrt{3}} < \alpha \leqslant \frac{\sqrt{3}-\sqrt{3}\cos(4\theta)-2\sqrt{7-4\cos(4\theta)+\cos^2(4\theta)}}{\cos(4\theta)-5}, \tag{7}$$

with $0 < \theta < \pi/4$. The detailed calculations are given in Appendixes A and B.

III. EXPERIMENTAL IMPLEMENTATION AND RESULTS

Figure 1 provides the schematic diagram of our experimental setup. The setup consists of three modules: (a) state preparation, (b) new state construction, and (c) entanglement detection. To be specific, a tunable diode laser emits a center wavelength of 405 nm and a high-power (130 mW) continuous laser beam, which passes through the polarization beam splitter (PBS). Subsequently, the transmitted beam is passed through a 405-nm half-wave plate (HWP1) and focused on two type-I β-barium borate (BBO) crystals ($6.0 \times 6.0 \times 0.5$ mm. The state $|\psi(\theta)\rangle = \cos(\theta)|HH\rangle + \sin(\theta)|VV\rangle$ shared by a pair of entangled photons ($\lambda = 810$ nm) is generated via spontaneous parametric down-conversion [40]. We can control the state parameter θ by adjusting the rotation angle of HWP1. We insert an unbalanced interferometer (UI0) in the path of A, and the 50/50 beam splitter (BS) in the UI0 separates the photon into two paths (represented by p_1 and p_2). In path p_1, the state of photons remains unchanged. Path p_2 is composed of HWP2 with 22.5° and three 2.6-mm yttrium orthovanadate (YVO_4) crystals, which can completely destroy the coherence. The state shared by the photons of path p_2 and path B in module (a) of Fig. 1 is transformed into an incoherent state in the basis of eigenvectors of the Pauli matrix σ_z, and the diagonal elements are $\cos^2\theta/2$, $\sin^2\theta/2$, $\cos^2\theta/2$, and $\sin^2\theta/2$, respectively. The two-qubit states $\rho_{AB}(\alpha,\theta)$ can be prepared by combining paths p_1 and p_2 into one, and the state parameter α can be conveniently changed by using the attenuator (ATT) in the UI0. Thirty states $\rho_{AB}(\alpha,\theta)$ are prepared to carry out the EPR steering test via entanglement detection in our experiment, and their distributions are denoted by the red, blue, and green solid circles in Fig. 2. Based on the theories of Refs. [36,37], the distributions of theoretically steerable states $\rho_{AB}(\alpha,\theta)$ are also displayed by different color regions. The red region represents the states $\rho_{AB}(\alpha,\theta)$ for which $\tau^1_{AB}(\alpha,\theta)$ and $\tau^2_{AB}(\alpha,\theta)$ are not entangled states. The results imply that the EPR steering in both directions cannot be determined through entanglement detection in theory. The cyan region, which is depicted by Eq. (7), represents the states $\rho_{AB}(\alpha,\theta)$ for which only $\tau^2_{AB}(\alpha,\theta)$ are entangled states. That is to say, only the EPR steering from Alice to Bob can be theoretically observed via entanglement detection, whether Bob can steer Alice cannot be determined. The green region represents the case that both $\tau^1_{AB}(\alpha,\theta)$ and $\tau^2_{AB}(\alpha,\theta)$ are entangled states, and the steering tasks theoretically succeed in both directions. In our method, we observe the EPR steering of 30 prepared states $\rho_{AB}(\alpha,\theta)$ by detecting the entanglement of the new states $\tau^1_{AB}(\alpha,\theta)$ and $\tau^2_{AB}(\alpha,\theta)$ without using any steering inequality or measurement setting. This is distinct from the scenarios in Ref. [33], which investigated the EPR steering of $\rho_{AB}(\alpha,\theta)$ by using the multimeasurement settings and the steering radius.

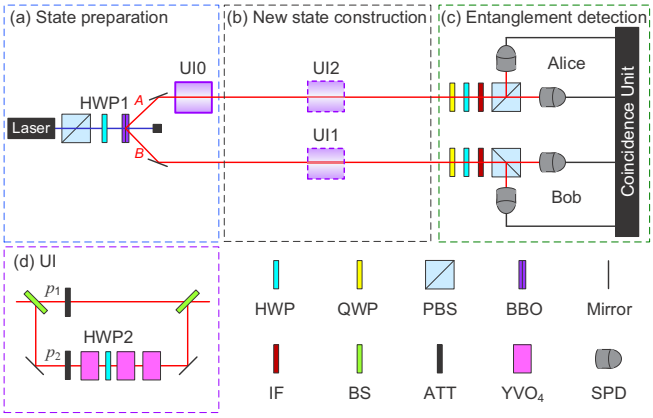

FIG. 1. Experimental setup. The setup includes three modules: (a) state preparation, (b) new state construction, and (c) entanglement detection. A family of two-qubit states $\rho_{AB}(\alpha,\theta)$ are prepared by the procession of a spontaneous parametric down-conversion and the unbalanced interferometer (UI0) in module (a). In module (b), two new states $\tau^1_{AB}(\alpha,\theta)$ and $\tau^2_{AB}(\alpha,\theta)$ from any $\rho_{AB}(\alpha,\theta)$ are constructed. If we only let the unbalanced interferometer (UI1) influence path B of module (b), and let path A remain unchanged, the state $\tau^1_{AB}(\alpha,\theta)$ can be prepared. On the contrary, if we let the unbalanced interferometer (UI2) influence path of module (b), and let path B remain unchanged, the state $\tau^2_{AB}(\alpha,\theta)$ can be generated. Module (c) is used to realize the entanglement detection of the new states. Abbreviations: HWP, half-wave plate; QWP, quarter-wave plate; PBS, polarizing beam splitter; BBO, type-I β-barium borate; IF, interference filter; BS, beam splitter; ATT, attenuator; YVO_4, yttrium orthovanadate crystal; SPD, single-photon detector.

Note that Fig. 2 also provides the distributions of the theoretically steerable states in the scenarios of two-measurement and three-measurement settings, which were experimentally verified in Ref. [33]. The red (blue) solid line and the dashed curve in Fig. 2 indicate the theoretical results by using two-measurement (three-measurement) settings and the steering radius. In the cases of two-measurement settings and the steering radius, the states below the red solid line are unsteerable. The states between the red solid line and the dashed curve are steerable from Alice to Bob in the case of two-measurement settings. The states above the red dashed curve can achieve the steering task in both directions for two-measurement settings. By employing three-measurement settings and the steering

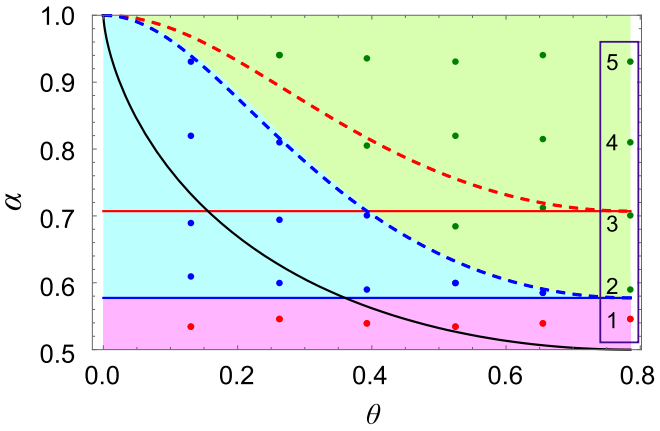

FIG. 2. Distributions of the prepared states $\rho_{AB}(\alpha,\theta)$ in our experiment and the theoretically steerable states in different scenarios. The red, blue, and green solid circles in the corresponding regions are the experimentally prepared states, and their steerability needs to be demonstrated via entanglement detection in our work. The red, cyan, and green areas represent the distributions of theoretically steerable states in the case of entanglement detection. The red (green) area corresponds to the states for which the EPR steering in both directions cannot (can) be theoretically demonstrated by detecting entanglement. The states located in the cyan area can only theoretically realize EPR steering from Alice to Bob in the scenario of entanglement detection, whether Bob can steer Alice cannot be determined. The red (blue) solid line and the red (blue) dashed curve are the theoretical results in the cases of two-measurement (three-measurement) settings and the steering radius [33]. Using the two-measurement settings and the steering radius, the states below the red solid line (above the red dashed curve) are theoretically unsteerable (both-way steerable) states. The states between the red solid line and the red dashed curve can only theoretically realize the EPR steering form Alice to Bob for two-measurement settings. Similarly, by using the three-measurement settings and the steering radius, the states below the blue solid line (above the blue dashed curve) are unsteerable (both-way steerable) in theory. The region between the blue solid line and the blue dashed curve represents the states that only the steering task from Alice to Bob can be theoretically achieved in the case of three-measurement settings. By using infinite-measurement settings [38], the states below (above) the black curve are steerable from Alice to Bob (both-way steerable).

radius, the states below the blue solid line (above the blue dashed curve) cannot (can) realize the EPR steering in both directions. The states between the blue solid line and the dashed curve are demonstrated to be steerable from Alice to Bob through three-measurement settings. In comparison with the two-measurement settings, the scenario of entanglement detection can capture more steerable states. Additionally, the green region (detectable both-way steerability by using entanglement detection) does not exactly coincide with the region above the blue dashed line (detectable both-way steerability by using three-measurement settings). However, it can be found that the scenario of entanglement detection is approximately equal to the three-measurement settings in the detection of both-way steerability. We also depict the inner bound described by $\cos^2(2\theta) = (2\alpha-1)/(2-\alpha)\alpha^3$ for the border of steering from Bob to Alice as the black solid curve shown in Fig. 2. The states below the curve can only realize steering from Alice to Bob by using infinite-measurement settings [38,41].

Next let us construct states $\tau^1_{AB}(\alpha,\theta)$ and $\tau^2_{AB}(\alpha,\theta)$ in our all-optical setup, as shown in module (b) of Fig. 1. To construct $\tau^1_{AB}(\alpha,\theta)$, we block path p_2 in UI2, and only let the unbalanced interferometer (UI1) influence path B. In other words, we let the photon of path B in module (b) be sent to UI1 and then sent to Bob. The photon of path A is sent to Alice directly. The photon state of path p_1 in UI1 remains unchanged. The state shared by path p_2 in UI1 and path A is dephased into an incoherent state, and the weights in bases of $|HH\rangle\langle HH|$, $|HV\rangle\langle HV|$, $|VH\rangle\langle VH|$, and $|VV\rangle\langle VV|$ are $(1+\alpha\cos 2\theta)/4$, $(1+\alpha\cos 2\theta)/4$, $(1-\alpha\cos 2\theta)/4$, and $(1-\alpha\cos 2\theta)/4$, respectively. The $\tau^1_{AB}(\alpha,\theta)$ can be constructed by combining the two paths p_1 and p_2 (in UI1) into one in the experiment. The state parameter μ_1 is set to $1/\sqrt{3}\approx 0.58$ by adjusting the ATT in UI1. The detailed method for determining μ_1 is shown in Appendixes A and B. Similarly, in order to construct $\tau^2_{AB}(\alpha,\theta)$, we need to block path p_2 in UI1 and let UI2 influence path A. That is, the photon of path B in module (b) is sent to Bob directly, and the photon of path A is sent to UI2 and then sent to Alice. The two-photon state shared by the photons in path p_2 of UI2 and path B is transformed into an incoherent state; the diagonal elements are $\cos^2\theta/2$, $\sin^2\theta/2$, $\cos^2\theta/2$, and $\sin^2\theta/2$, respectively. The state $\tau^2_{AB}(\alpha,\theta)$ can be constructed by mixing paths p_1 and p_2 of UI2 into one. The state parameter μ_2 is also set to $1/\sqrt{3}\approx 0.58$ by using the ATT in UI2. Module (c) of Fig. 1 is used to realize the detection of entanglement by performing a quantum state tomography process [42]. The fidelity of $\tau^1_{AB}(\alpha,\theta)$ and $\tau^2_{AB}(\alpha,\theta)$ are calculated by $F(\tau,\tau_0)\equiv \mathrm{tr}\sqrt{\sqrt{\tau}\tau_0\sqrt{\tau}}$ [43], where τ and τ_0 are the experimental and theoretical density matrices, respectively. In our experiment, 30 states $\tau^1_{AB}(\alpha,\theta)$ and 30 states $\tau^2_{AB}(\alpha,\theta)$ are constructed, and the fidelities of all these states are beyond 0.9873.

In the following, we observe the EPR steering by detecting the entanglement of these 60 states. The results of the experiment are shown in Fig. 3, and the insets in Figs. 3(e) and 3(f) are the magnifications of the regions in the purple panes. The solid circles and hollow triangles represent the experimental results of $C(\tau^1_{AB}(\alpha,\theta))$ and $C(\tau^2_{AB}(\alpha,\theta))$, respectively, which are calculated according to the density matrices $\tau^1_{AB}(\alpha,\theta)$ and $\tau^2_{AB}(\alpha,\theta)$ obtained by quantum state tomography. Based on the standard deviation from the statistical variation of the photon counts, which are assumed to follow Poisson distribution, all error bars are estimated in the experiment. Note that some of the error bars are very small and are not displayed in Fig. 3. In order to make the experimental results correspond to the prepared states in Fig. 2, we use solid circles and hollow triangles with different colors in Fig. 3 to represent the corresponding experimental results. As seen from Fig. 3, the 6 red solid circles and 6 red hollow triangles display that the experimental states $\tau^1_{AB}(\alpha,\theta)$ and $\tau^2_{AB}(\alpha,\theta)$ are all separable. The results certify that the EPR steering of 6 prepared states $\rho_{AB}(\alpha,\theta)$ (represented by 6 red solid circles in Fig. 2) cannot be observed via the detection of entanglement. The 11 blue solid circles and 11 blue hollow

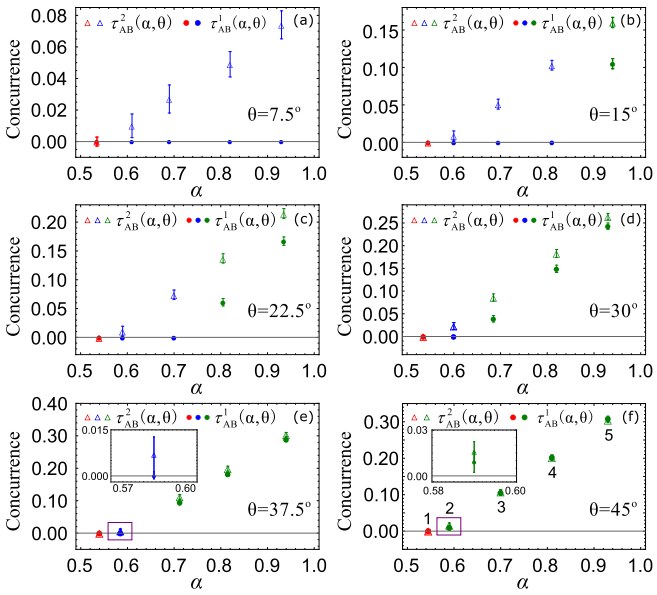

FIG. 3. The experimental results. The solid circles and the hollow triangles represent the experimental results of $C(\tau^1_{AB}(\alpha,\theta))$ and $C(\tau^2_{AB}(\alpha,\theta))$, respectively. The red solid circles and hollow triangles correspond to the results that the $\tau^1_{AB}(\alpha,\theta)$ and $\tau^2_{AB}(\alpha,\theta)$ are all separated; i.e., the EPR steering of $\rho_{AB}(\alpha,\theta)$ cannot be verified through entanglement detection. The blue solid circles and hollow triangles correspond to the case for which only the $\tau^2_{AB}(\alpha,\theta)$ is entangled, namely, only the steering from Alice to steer Bob can be observed via entanglement detection. The green solid circles and hollow triangles correspond to the results that $\tau^1_{AB}(\alpha,\theta)$ and $\tau^2_{AB}(\alpha,\theta)$ are all entangled; i.e., Alice and Bob can steer each other. Some of error bars are very small and not shown.

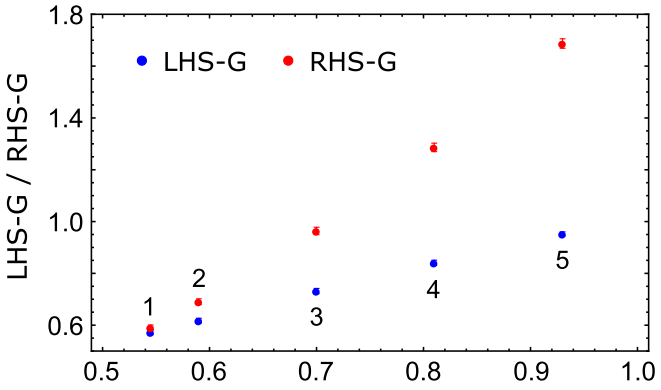

FIG. 4. The experimental results for $\rho_{AB}(\alpha,\pi/4)$ through the geometric Bell-like steering inequality. The blue and red solid circles denote the left-hand side (LHS-G) and the right-hand side (RHS-G) of the geometric Bell-like steering inequality, respectively. The experimental data labeled by 1, 2, 3, 4, and 5 correspond to the test results of states labeled by 1, 2, 3, 4, and 5 in Fig. 2, respectively. Some of the error bars are too small to display.

triangles in Fig. 3 represent that the $\tau^1_{AB}(\alpha,\theta)$ are separable states and the $\tau^2_{AB}(\alpha,\theta)$ are entangled states, respectively. The experimental results can help us to identify that the 11 prepared states $\rho_{AB}(\alpha,\theta)$ (represented by 11 blue solid circles in Fig. 2) can realize the EPR steering from Alice to Bob, and whether Bob can steer Alice cannot be decided in this scenario. Hence, the results do not imply that the 11 prepared states are one-way steering (namely, Alice can steer Bob's state but Bob cannot steer Alice's state). One can see from Fig. 3 that the 13 green solid circles and 13 green hollow triangles indicate that the $\tau^1_{AB}(\alpha,\theta)$ and $\tau^2_{AB}(\alpha,\theta)$ states are all entangled states in the experiment. The results verify that the 13 prepared states $\rho_{AB}(\alpha,\theta)$ (represented by 13 green solid circles in Fig. 2) are both-way steering states, in which the steering tasks succeed in both directions (Alice and Bob can steer each other). Hence, the experimental results show good agreement with the theoretical predictions in Fig. 2, and the EPR steering of the two-qubit states $\rho_{AB}(\alpha,\theta)$ can be observed through the entanglement detection of these new states. As shown in Fig. 2, some steerable states (the states between the red solid line and the blue solid line), which can be demonstrated in our scenario, cannot be verified in the case of two-setting projective measurements. Nearly all steerable states (the states above the blue solid line), which can be observed in the case of three-setting projective measurements, can be witnessed by detecting entanglement. This means that the ability to detect the EPR steering in our strategy is stronger than that of two-measurement settings and can compete with the three-measurement settings.

In order to further verify the effectiveness of our scenario, we take the EPR steering of $\rho_{AB}(\alpha,\pi/4)$ (labeled by 1, 2, 3, 4, and 5 in Fig. 2) by using the geometric Bell-like steering inequality as an example, which is denoted by $\mathrm{Max}_{\vec{m},\vec{n}} E_Q(\vec{m},\vec{n}) \geqslant 2(\sum_{i,j=1}^{3} T_{ij}^2)/3$ [19]. Here, $\vec{m}\cdot\vec{\sigma}^A$ and $\vec{n}\cdot\vec{\sigma}^B$ are projective measurements implemented by Alice and Bob, respectively. $\vec{\sigma}^A$ and $\vec{\sigma}^B$ are Pauli matrices, and $T_{ij} = \mathrm{tr}[\rho_{\mathrm{AB}}(\sigma_i^{\mathrm{A}} \otimes \sigma_j^{\mathrm{B}})]$ is the matrix element of the spin correlation matrix. We use LHS-G and RHS-G to represent the left-hand side and the right-hand side of the geometric Bell-like steering inequality, respectively. Note that, the state $\rho_{AB}(\alpha,\pi/4)$ corresponds to the Werner state [44]. It is well known that the state is steerable from Alice to Bob in the case of $\alpha > 1/2$, and Bob can steer Alice for $\alpha > 1/2$ [3,45]. Based on the quantum state tomography, the experimental LHS-G and RHS-G are calculated according to the density matrix of $\rho_{AB}(\alpha,\pi/4)$ (the fidelities of all these states are higher than 0.9893). The experimental results are shown in Fig. 4. The both-way steering of the states labeled by 2, 3, 4, and 5 in Fig. 2 can be observed in our scenario [see Fig. 3(f)], and these states also violate the geometric Bell-like steering inequality (the data of LHS-G are less than the data of RHS-G, see Fig. 4). The results further verify that the entanglement detection of newly constructed states can effectively witness the EPR steering in experiments. Meanwhile, it is worth noting that the EPR steering of the state labeled by 1 in Fig. 2 can be observed by employing the geometric Bell-like steering inequality; however, it cannot be observed through our scenario. The reason is that the ability of geometric Bell-like steering inequality to detect the EPR steering of the Werner state (for $\alpha > 1/2$ [19,35]) is stronger than the scenario of entanglement detection (for $\alpha > 1/\sqrt{3}$).

IV. CONCLUSIONS

In this paper, based on 30 prepared two-qubit states $\rho_{AB}(\alpha,\theta)$, 60 states $\tau^1_{AB}(\alpha,\theta)$ and $\tau^2_{AB}(\alpha,\theta)$ are constructed in the experiment. The EPR steering of $\rho_{AB}(\alpha,\theta)$ are experimentally observed by detecting the entanglement of these newly constructed states, and any steering inequality and measurement setting are not used in the process of demonstration. Our results verify that the steering from Bob to Alice can be witnessed by the entanglement of $\tau^1_{AB}(\alpha,\theta)$, and the steering from Alice to Bob can be witnessed by the entanglement of $\tau^2_{AB}(\alpha,\theta)$. Hence, the entanglement of newly constructed states provides a way to witness the EPR steering in experiments. The ability to testing the EPR steering in our scenario is stronger than that of the two-setting projective measurements, and more steerable states can be observed by detecting the entanglement of the constructed states. Consequently, our work demonstrates that one can effectively certify the EPR steering by translating it into an easily certified quantum nonlocality (i.e., the entanglement) in experiments, and it is also potentially used to understand the relation between steering and entanglement in quantum information tasks.

ACKNOWLEDGMENTS

This work was supported by the National Natural Science Foundation of China (Grants No. 11575001, No. 61601002, and No. 11605028), the Program for Excellent Talents in University of Anhui Province of China (Grant No. gxyq2018059), the Natural Science Research Project of Education Department of Anhui Province of China (Grants No. KJ2018A0343, No. KJ2017A406, and No. KJ2017A401), the Open Foundation for CAS Key Laboratory of Quantum Information under Grants No. KQI201801 and No. KQI201804, and the Key Program of Excellent Youth Talent Project of the Education Department of Anhui Province of China under Grant No. gxyqZD2018065.

H.Y. and Z.Y.D. contributed equally to this work.

APPENDIX A: THE EPR STEERING CONDITION FOR $\rho_{AB}(\alpha,\theta)$ BASED ON THE ENTANGLEMENT DETECTION

Considering a two-qubit state ρ_{AB}, the concurrence is written as $C(\rho_{AB}) = \max\{0, \sqrt{\lambda_1} - \sqrt{\lambda_2} - \sqrt{\lambda_3} - \sqrt{\lambda_4}\}$ [39], where λ_i $(i = 1, 2, 3, 4)$ are the eigenvalues with decreasing order of the matrix $\rho_{AB}(\sigma_y \otimes \sigma_y)\rho^*_{AB}(\sigma_y \otimes \sigma_y)$. The variable ρ^*_{AB} represents the complex conjugate of ρ_{AB} in the fixed basis $\{|00\rangle, |01\rangle, |10\rangle, |11\rangle\}$. For the two-qubit X states ρ^X_{AB}, the concurrence can be derived in a simple form [46]:

$$C(\rho^X_{AB}) = 2\max\left\{0, \sqrt{\rho^X_{14}\rho^X_{41}} - \sqrt{\rho^X_{22}\rho^X_{33}}, \sqrt{\rho^X_{23}\rho^X_{32}} - \sqrt{\rho^X_{11}\rho^X_{44}}\right\}. \tag{A1}$$

According to Eqs. (4) and (A1), the concurrence of $\tau^1_{AB}(\alpha,\theta)$ is obtained by

$$C\left(\tau^1_{AB}(\alpha,\theta)\right) = 2\max\left\{0, C^1_{AB1}, C^2_{AB1}\right\}, \tag{A2}$$

with

$$C^1_{AB1} = \frac{2\alpha\sqrt{1-\cos(4\theta)} - \sqrt{5-\alpha(2\sqrt{3}+\alpha) - (\sqrt{3}\alpha-1)^2\cos(4\theta)}}{4\sqrt{6}} \tag{A3}$$

and

$$C^2_{AB1} = -\frac{\sqrt{5+\alpha(2\sqrt{3}-\alpha) - (\sqrt{3}\alpha+1)^2\cos(4\theta)}}{4\sqrt{6}}. \tag{A4}$$

The condition of the EPR steering from Bob to Alice is $C[\tau^1_{AB}(\alpha,\theta)] > 0$. Then the conditions can be given by $0 < \theta \leqslant \pi/4$ and

$$\frac{\sqrt{3} - \sqrt{3}\cos(4\theta) - 2\sqrt{7 - 4\cos(4\theta) + \cos^2(4\theta)}}{\cos(4\theta) - 5} < \alpha \leqslant 1. \tag{A5}$$

Similarly, the concurrence of $\tau^2_{AB}(\alpha,\theta)$ is expressed as

$$C\left(\tau^2_{AB}(\alpha,\theta)\right) = 2\max\left\{0, C^1_{AB2}, C^2_{AB2}\right\}, \tag{A6}$$

where

$$C^1_{AB2} = \frac{(3\alpha - \sqrt{3})\sin(2\theta)}{4\sqrt{3}} \tag{A7}$$

and

$$C^2_{AB2} = -\frac{(\sqrt{3}+\alpha)\sin(2\theta)}{4\sqrt{3}}. \tag{A8}$$

The condition of the EPR steering from Alice to Bob is $C(\tau^2_{AB}(\alpha,\theta)) > 0$, which can be easily derived as $1/\sqrt{3} < \alpha \leqslant 1$ and $0 < \theta \leqslant \pi/4$. Hence, we obtain the condition for the case that $\tau^2_{AB}(\alpha,\theta)$ is an entangled state and $\tau^1_{AB}(\alpha,\theta)$ is a separable state, i.e.,

$$\frac{1}{\sqrt{3}} < \alpha \leqslant \frac{\sqrt{3} - \sqrt{3}\cos(4\theta) - 2\sqrt{7 - 4\cos(4\theta) + \cos^2(4\theta)}}{\cos(4\theta) - 5}, \tag{A9}$$

with $0 < \theta < \pi/4$.

APPENDIX B: THE METHOD TO DETERMINE THE EXPERIMENTAL PARAMETERS μ_1 AND μ_2

As seen from Fig. 1 in the main text, we block path p_2 in UI2 and let the photon of path A in module (b) be sent to Alice directly. Meanwhile, we let the photon of path B in module (b) be sent to UI1 and then sent to Bob. The state of path p_1 in UI1 remains unchanged, i.e., $\rho^{\mathrm{UI1}}_{p_1}(\alpha,\theta) = \rho_{AB}(\alpha,\theta)$. The state of

path p_2 in UI1 can be written as

$$\rho_{p_2}^{\mathrm{UI1}}(\alpha,\theta) = \frac{1+\alpha\cos 2\theta}{4}|HH\rangle\langle HH| + \frac{1+\alpha\cos 2\theta}{4}|HV\rangle\langle HV| + \frac{1-\alpha\cos 2\theta}{4}|VH\rangle\langle VH| + \frac{1-\alpha\cos 2\theta}{4}|VV\rangle\langle VV|. \quad \text{(B1)}$$

Combining paths p_1 and p_2 into one, the state $\tau_{AB}^1(\alpha,\theta)$ can be prepared. The mixed parameter μ_1 in $\tau_{AB}^1(\alpha,\theta)$ is determined as follows.

We denote a set of measurement bases as $M = \{|HH\rangle\langle HH|, |HV\rangle\langle HV|, |VH\rangle\langle VH|, |VV\rangle\langle VV|\}$. First, we block path p_2 in UI1 and implement a set of measurements in the basis of M. The corresponding coincidence counts are labeled as M_1^1, M_2^1, M_3^1, and M_4^1, and the total photon count is $C_1^1 = M_1^1 + M_2^1 + M_3^1 + M_4^1$. Second, we block path p_1 in UI1. After performing a complete measurement in the basis of M, the corresponding coincidence counts are denoted as N_1^1, N_2^1, N_3^1, and N_4^1. The total photon count is $C_2^1 = N_1^1 + N_2^1 + N_3^1 + N_4^1$. Finally, The mixed parameter μ_1 is obtained by $\mu_1 = C_1^1/(C_1^1 + C_2^1)$.

Similarly, the parameter μ_2 in the state $\tau_{AB}^2(\alpha,\theta)$ can be determined. As shown in Fig. 1 in the main text, we block path p_2 in UI1 and let the photon of path B in module (b) be sent to Bob directly. Meanwhile, we let the photon of path A in module (b) be sent to UI2 and then sent to Alice. The state of path p_1 in UI2 remains unchanged, i.e., $\rho_{p_1}^{\mathrm{UI2}}(\alpha,\theta) = \rho_{AB}(\alpha,\theta)$. The state of path p_2 in UI2 is transformed into

$$\rho_{p_2}^{\mathrm{UI2}}(\alpha,\theta) = \frac{\cos^2\theta}{2}|HH\rangle\langle HH| + \frac{\sin^2\theta}{2}|HV\rangle\langle HV| + \frac{\cos^2\theta}{2}|VH\rangle\langle VH| + \frac{\sin^2\theta}{2}|VV\rangle\langle VV|. \quad \text{(B2)}$$

We construct the state $\tau_{AB}^2(\alpha,\theta)$ by combining paths p_1 and p_2 mentioned above into one. The mixed parameter μ_2 can be obtained as follows. We block path p_2 in UI2 and carry out a set of measurements in the basis of M. The photon counts are labeled as M_1^2, M_2^2, M_3^2, and M_4^2, and the total photon count is $C_1^2 = M_1^2 + M_2^2 + M_3^2 + M_4^2$. Then, we block path p_1 in UI2 and implement a complete measurement in the basis M; the corresponding coincidence counts are written as N_1^2, N_2^2, N_3^2, and N_4^2. The total photon coincidence count is $C_2^2 = N_1^2 + N_2^2 + N_3^2 + N_4^2$, and the parameter μ_2 is determined by $\mu_2 = C_1^2/(C_1^2 + C_2^2)$.

[1] A. Einstein, B. Podolsky, and N. Rosen, Can quantum-mechanical description of physical reality be considered complete? Phys. Rev. **47**, 777 (1935).

[2] E. Schrödinger, Discussion of probability relations between separated systems, Math. Proc. Cambridge Philos. Soc. **31**, 555 (1935).

[3] H. M. Wiseman, S. J. Jones, and A. C. Doherty, Steering, Entanglement, Nonlocality, and the Einstein-Podolsky-Rosen Paradox, Phys. Rev. Lett. **98**, 140402 (2007).

[4] R. Horodecki, P. Horodecki, M. Horodecki, and K. Horodecki, Quantum entanglement, Rev. Mod. Phys. **81**, 865 (2009).

[5] J. S. Bell, On the Einstein Podolsky Rosen paradox, Physics **1**, 195 (1965).

[6] N. Brunner, D. Cavalcanti, S. Pironio, V. Scarani, and S. Wehner, Bell nonlocality, Rev. Mod. Phys. **86**, 419 (2014).

[7] C. Branciard, E. G. Cavalcanti, S. P. Walborn, V. Scarani, and H. M. Wiseman, One-sided device-independent quantum key distribution: Security, feasibility, and the connection with steering, Phys. Rev. A **85**, 010301(R) (2012).

[8] T. Gehring, V. Händchen, J. Duhme, F. Furrer, T. Franz, C. Pacher, R. F. Werner, and R. Schnabel, Implementation of continuous-variable quantum key distribution with composable and one-sided-device independent security against coherent attacks, Nat. Commun. **6**, 8795 (2015).

[9] N. Walk, S. Hosseini, J. Geng, O. Thearle, J. Y. Haw, S. Armstrong, S. M. Assad, J. Janousek, T. C. Ralph, T. Symul, H. M. Wiseman, and P. K. Lam, Experimental demonstration of Gaussian protocols for one-sided device-independent quantum key distribution, Optica **3**, 634 (2015).

[10] M. D. Reid, Signifying quantum benchmarks for qubit teleportation and secure quantum communication using Einstein-Podolsky-Rosen steering inequalities, Phys. Rev. A **88**, 062338 (2013).

[11] Q. He, L. Rosales-Zárate, G. Adesso, and M. D. Reid, Secure Continuous Variable Teleportation and Einstein-Podolsky-Rosen Steering, Phys. Rev. Lett. **115**, 180502 (2015).

[12] P. Skrzypczyk and D. Cavalcanti, Maximal Randomness Generation from Steering Inequality Violations Using Qudits, Phys. Rev. Lett. **120**, 260401 (2018).

[13] E. G. Cavalcanti, S. J. Jones, H. M. Wiseman, and M. D. Reid, Experimental criteria for steering and the Einstein-Podolsky-Rosen paradox, Phys. Rev. A **80**, 032112 (2009).

[14] M. F. Pusey, Negativity and steering: A stronger Peres conjecture, Phys. Rev. A **88**, 032313 (2013).

[15] S. P. Walborn, A. Salles, R. M. Gomes, F. Toscano, and P. H. Souto Ribeiro, Revealing Hidden Einstein-Podolsky-Rosen Nonlocality, Phys. Rev. Lett. **106**, 130402 (2011).

[16] J. Schneeloch, C. J. Broadbent, S. P. Walborn, E. G. Cavalcanti, and J. C. Howell, Einstein-Podolsky-Rosen steering inequalities from entropic uncertainty relations, Phys. Rev. A **87**, 062103 (2013).

[17] T. Kriváchy, F. Fröwis, and N. Brunner, Tight steering inequalities from generalized entropic uncertainty relations, Phys. Rev. A **98**, 062111 (2018).

[18] A. C. S. Costa, R. Uola, and O. Gühne, Steering criteria from general entropic uncertainty relations, Phys. Rev. A **98**, 050104(R) (2018).

[19] M. Żukowski, A. Dutta, and Z. Yin, Geometric Bell-like inequalities for steering, Phys. Rev. A **91**, 032107 (2015).

[20] A. Rutkowski, A. Buraczewski, P. Horodecki, and M. Stobińska, Quantum Steering Inequality with Tolerance for Measurement-Setting Errors: Experimentally Feasible Signa-

ture of Unbounded Violation, Phys. Rev. Lett. **118**, 020402 (2017).

[21] D. A. Evans and H. M. Wiseman, Optimal measurements for tests of Einstein-Podolsky-Rosen steering with no detection loophole using two-qubit Werner states, Phys. Rev. A **90**, 012114 (2014).

[22] M. T. Quintino, T. Vértesi, D. Cavalcanti, R. Augusiak, M. Demianowicz, A. Acín, and N. Brunner, Inequivalence of entanglement, steering, and Bell nonlocality for general measurements, Phys. Rev. A **92**, 032107 (2015).

[23] P. Skrzypczyk, M. Navascués, and D. Cavalcanti, Quantifying Einstein-Podolsky-Rosen Steering, Phys. Rev. Lett. **112**, 180404 (2014).

[24] S. Wollmann, N. Walk, A. J. Bennet, H. M. Wiseman, and G. J. Pryde, Observation of Genuine One-Way Einstein-Podolsky-Rosen Steering, Phys. Rev. Lett. **116**, 160403 (2016).

[25] S. L. W. Midgley, A. J. Ferris, and M. K. Olsen, Asymmetric Gaussian steering: When Alice and Bob disagree, Phys. Rev. A **81**, 022101 (2010).

[26] M. K. Olsen, Asymmetric Gaussian harmonic steering in second-harmonic generation, Phys. Rev. A **88**, 051802(R) (2013).

[27] K. Rosołek, M. Stobińska, M. Wieśniak, and M. Żukowski, Two Copies of the Einstein-Podolsky-Rosen State of Light Lead to Refutation of EPR Ideas, Phys. Rev. Lett. **114**, 100402 (2015).

[28] D. J. Saunders, S. J. Jones, H. M. Wiseman, and G. J. Pryde, Experimental EPR-steering using Bell-local states, Nat. Phys. **6**, 845 (2010).

[29] A. J. Bennet, D. A. Evans, D. J. Saunders, C. Branciard, E. G. Cavalcanti, H. M. Wiseman, and G. J. Pryde, Arbitrarily Loss-Tolerant Einstein-Podolsky-Rosen Steering Allowing a Demonstration over 1 km of Optical Fiber with No Detection Loophole, Phys. Rev. X **2**, 031003 (2012).

[30] V. Händchen, T. Eberle, S. Steinlechner, A. Samblowski, T. Franz, R. F. Werner, and R. Schnabel, Observation of one-way Einstein-Podolsky-Rosen steering, Nat. Photonics **6**, 596 (2012).

[31] S. Armstrong, M. Wang, R. Y. Teh, Q. Gong, Q. He, J. Janousek, H. A. Bachor, M. D. Reid, and P. K. Lam, Multipartite Einstein-Podolsky-Rosen steering and genuine tripartite entanglement with optical networks, Nat. Phys. **11**, 167 (2015).

[32] K. Sun, X. J. Ye, J. S. Xu, X. Y. Xu, J. S. Tang, Y. C. Wu, J. L. Chen, C. F. Li, and G. C. Guo, Experimental Quantification of Asymmetric Einstein-Podolsky-Rosen Steering, Phys. Rev. Lett. **116**, 160404 (2016).

[33] Y. Xiao, X. J. Ye, K. Sun, J. S. Xu, C. F. Li, and G. C. Guo, Demonstration of Multisetting One-Way Einstein-Podolsky-Rosen Steering in Two-Qubit Systems, Phys. Rev. Lett. **118**, 140404 (2017).

[34] N. Tischler, F. Ghafari, T. J. Baker, S. Slussarenko, R. B. Patel, M. M. Weston, S. Wollmann, L. K. Shalm, V. B. Verma, S. W. Nam, H. C. Nguyen, H. M. Wiseman, and G. J. Pryde, Conclusive Experimental Demonstration of One-Way Einstein-Podolsky-Rosen Steering, Phys. Rev. Lett. **121**, 100401 (2018).

[35] J. Li, C. Y. Wang, T. J. Liu, and Q. Wang, Experimental verification of steerability via geometric Bell-like inequalities, Phys. Rev. A **97**, 032107 (2018).

[36] D. Das, S. Sasma, and S. Roy, Detecting Einstein-Podolsky-Rosen steering through entanglement detection, Phys. Rev. A **99**, 052109 (2019).

[37] C. Chen, C. Ren, X. J. Ye, and J. L. Chen, Mapping criteria between nonlocality and steerability in qudit-qubit systems and between steerability and entanglement in qubit-qudit systems, Phys. Rev. A **98**, 052114 (2018).

[38] J. Bowles, F. Hirsch, M. T. Quintino, and N. Brunner, Sufficient criterion for guaranteeing that a two-qubit state is unsteerable, Phys. Rev. A **93**, 022121 (2016).

[39] W. K. Wootters, Entanglement of Formation of an Arbitrary State of Two Qubits, Phys. Rev. Lett. **80**, 2245 (1998).

[40] P. G. Kwiat, E. Waks, A. G. White, I. Appelbaum, and P. H. Eberhard, Ultrabright source of polarization-entangled photons, Phys. Rev. A **60**, R773 (1999).

[41] R. Uola, A. C. S. Costa, H. C. Nguyen, and O. Gühne, Quantum steering, Rev. Mod. Phys. **92**, 015001 (2020).

[42] D. F. V. James, P. G. Kwiat, W. J. Munro, and A. G. White, Measurement of qubits, Phys. Rev. A **64**, 052312 (2001).

[43] M. A. Nielsen and I. L. Chuang, *Quantum Computation and Quantum Information* (Cambridge University, Cambridge, England, 2000).

[44] R. F. Werner, Quantum states with Einstein-Podolsky-Rosen correlations admitting a hidden-variable model, Phys. Rev. A **40**, 4277 (1989).

[45] F. Hirsch, M. T. Quintino, T. Vértesi, M. F. Pusey, and N. Brunner, Algorithmic Construction of Local Hidden Variable Models for Entangled Quantum States, Phys. Rev. Lett. **117**, 190402 (2016).

[46] J. Maziero, T. Werlang, F. F. Fanchini, L. C. Céleri, and R. M. Serra, System-reservoir dynamics of quantum and classical correlations, Phys. Rev. A **81**, 022116 (2010).